Original Article Kuanxiong aerosol attenuates post-myocardial infarction heart failure by immune modulation via the NOTCH1 pathway

Zhifei Sun^{1,2,3,4,5,6}, Xiaoding Wang⁶, Zhong Xu⁷, Li Xin⁶, Weidong Sun⁶, Meng Ning^{2,3,4,5}, Yingwu Liu^{1,2,3,4,5}

¹The Third Central Clinical College of Tianjin Medical University, Tianjin 300170, P. R. China; ²Tianjin Key Laboratory of Extracorporeal Life Support for Critical Diseases, Tianjin 300170, P. R. China; ³Artificial Cell Engineering Technology Research Center, Tianjin 300170, P. R. China; ⁴Tianjin Institute of Hepatobiliary Disease, Tianjin 300170, P. R. China; ⁵Department of Heart Center, Tianjin Third Central Hospital, Tianjin 300170, P. R. China; ⁵Department of Cardiovascular Medicine, The Affiliated Tai'an Central Hospital of Qingdao University, Tai'an 271000, Shandong, P. R. China; ⁵Department of Cardiovascular Medicine, The Affiliated Tai'an Central Hospital of Qingdao University, Tai'an 271000, Shandong, P. R. China

Received May 30, 2025; Accepted August 30, 2025; Epub September 15, 2025; Published September 30, 2025

Abstract: Objective: To investigate the mechanisms underlying the therapeutic effects of Kuanxiong aerosol (KXA) in heart failure after myocardial infarction (HFAMI). Methods: A HFAMI rat model was established. Echocardiography, H&E and TUNEL staining of heart tissue, and ELISA for HFAMI-related biomarkers were performed after KXA treatment. qPCR, Western blot, and flow cytometry were used to identify potential KXA targets in vivo and in vitro. Cell viability and apoptosis were evaluated using the Cell Counting Kit-8. Results: KXA significantly decreased left ventricular end diastolic diameter (LVIDD, 6.49 \pm 0.40 mm, P<0.001) and left ventricular end-systolic dimension (LVISD, 3.72 \pm 0.27 mm, P<0.001), while increasing left ventricular ejection fraction (LVEF, 64.66 \pm 2.69%, P<0.001) and left ventricular fraction shortening (LVFS, 43.20 \pm 5.93%, P<0.001). KXA also suppressed cardiomyocyte apoptosis and reduced levels of NT-proBNP, ST2, IL-6, TNF- α , MMP2, and MMP9 (all P<0.05). Additionally, KXA reduced immune cell infiltration (Neutrophils, Macrophages, Th1, NK cells) and upregulated DLL4, NOTCH1, NICD, and Hes1 expression in the infarction zone. In doxorubicin-treated cells, KXA enhanced cell viability and upregulated Bcl-2, Bcl-xL, and NOTCH pathway proteins, while reducing cleaved caspase-3 (all P<0.05). Conclusion: KXA improves HFAMI by modulating immune responses and activating the NOTCH1 signaling pathway.

Keywords: Myocardial infarction, heart failure, Kuanxiong aerosol, immunomodulation, NOTCH1 pathway, pharmacology

Introduction

Coronary heart disease continues to be a leading cause of mortality in both developed and developing countries, with myocardial infarction (MI) being one of the most severe forms, contributing significantly to death among coronary heart disease patients [1]. Heart failure (HF) is a major complication following MI, occurring when the heart's structure and function are severely impaired. Approximately 25% of MI survivors will develop HF within one year post-discharge, which significantly increases the risk of mortality and worsens prognosis [2, 3]. The 30-day mortality rate for newly diagnosed HF is around 10%, while the 5-year mortality rate can

be as high as 45%-60% [4]. Despite advances in therapies like percutaneous coronary intervention and pharmacological treatments (e.g., SGLT2 inhibitors, ARNI), the complexity of heart failure after myocardial infarction (HFAMI) still poses significant clinical challenges due to limitations of single-target treatments and insufficient efficacy [5]. Therefore, novel therapeutic approaches involving immune regulation and multi-target interventions using Chinese herbal medicine are emerging as promising strategies for HFAMI management.

Traditional Chinese Medicine (TCM) has been utilized for centuries in the management of HF [6]. However, the exact mechanisms underlying

TCM's therapeutic effects in preventing and treating HF remain incompletely understood, largely due to the absence of robust, largescale clinical trials and modern mechanistic studies. Despite this, recent pharmacological and molecular advancements have begun to unravel the cardioprotective actions of TCM, including modulation of ventricular remodeling, suppression of systemic inflammation, improvement of cardiac energy metabolism, and regulation of neurohormonal activation [7, 8]. For instance, Ginseng Dingzhi Decoction (GN), a classical TCM formulation, has been reported to alleviate HF progression and protect cardiomyocytes by restoring intestinal microbiota balance and enhancing mitochondrial function [9]. Similarly, Yang et al. demonstrated that Linggui Zhugan Decoction attenuates ventricular remodeling in rats with HFAMI, a mechanism associated with the inhibition of the Wnt/Bcatenin signaling pathway, which plays a key role in myocardial fibrosis and adverse cardiac remodeling [10].

Kuanxiong aerosol (KXA) is a well-known TCM formulation composed of five medicinal herbs: the volatile oil from Asarum sieboldii Mig. (Xixin), Alpinia officinarum Hance (Gaoliangjiang), Santalum album L. (Tanxiang), Piper longum L. (Bibo), and Borneolum (Bingpian) [11]. Clinical evidence suggests that KXA exhibits anti-anginal effects comparable to conventional nitrate therapy, with a more favorable safety profile [12]. Modern pharmacological studies have further elucidated the multi-target mechanisms underlying KXA's cardioprotective effects, which include potent vasodilation through nitric oxide-mediated pathways, amelioration of myocardial ischemia-reperfusion injury, neuroprotective effects in ischemic stroke models, and inhibition of cardiomyocyte apoptosis through modulation of Bcl-2/Bax signaling [13-15]. Despite these promising results, the therapeutic potential of KXA in HFAMI has not been fully explored.

Following MI, extensive cardiomyocyte necrosis in the ischemic zone releases damage-associated molecular patterns (DAMPs) that activate the innate immune system through binding to pattern recognition receptors (PRRs) on macrophages, neutrophils, and dendritic cells. This triggers a robust inflammatory response, which is critical for both the progression of cardiac

injury and the development of HF [16-19]. Emerging research highlights the role of immune regulation in mitigating adverse ventricular remodeling and preventing HFAMI. Li et al. recently identified distinct immune cell profiles in acute MI versus chronic ischemic HF, underscoring the dynamic involvement of the immune system throughout disease progression [20]. These findings suggest that immunomodulation may offer a therapeutic avenue for HFAMI. However, whether KXA exerts cardioprotective effects through immune regulation remains an unresolved question that warrants further investigation.

The NOTCH signaling pathway is a key regulator of cellular homeostasis, influencing a wide range of biological processes such as embryonic development, cell proliferation and apoptosis, and tissue repair [21]. The pathway has been implicated in cardiovascular development and is known to promote the proliferation of immature myocardial cells [22]. Four NOTCH receptors (1-4) have been identified in mammals, all sharing similar tertiary structures but triggering distinct cellular responses [23]. NOTCH1 has been specifically implicated in cardiovascular disorders, particularly in protecting the heart during various stages of MI, including ischemic injury, the reactive phase, and myocardial scarring [24, 25]. For instance, Cui et al. reported that inhibition of AlkB homolog 5 (ALKBH5) alleviated hypoxia-induced pyroptosis in rat cardiac fibroblasts, modulating MI by reducing Notch1/NLRP3 inflammasome activation [26]. TCM compounds such as curcumin and gastrodin have been shown to alleviate brain tissue damage by inhibiting NOTCH1 signaling and reducing inflammatory cytokine release (e.g., TNF-α, IL-1β) [27]. Furthermore, Oishen Granules promote angiogenesis and protect against MI injury through the BMP2-DII4-Notch1 pathway [28]. Borneol, one of the components of KXA, has also been shown to exert neuroprotective effects by modulating the NOTCH pathway [29]. However, the potential role of KXA in modulating NOTCH1 signaling in HFAMI has yet to be explored.

We hypothesize that KXA alleviates post-MI HF through immune modulation via the NOTCH1 signaling pathway. This study will enrich the mechanistic understanding of TCM in cardio-vascular diseases and provide innovative therapeutic strategies for clinical intervention.

Materials and methods

Animals

Fifteen healthy, eight-week-old SPF-level SD rats were housed under controlled conditions (22°C ± 2°C, 40%-50% humidity, 12-hour light/dark cycle). After a one-week acclimatization period, rats were randomly assigned to the sham control (n=5) and experimental groups (n=10, including model and KXA groups) using a random number table (SPSS 26.0, seed=12345). The experimental group underwent left anterior descending coronary artery ligation to induce acute MI [30]. Accurate localization of LAD is critical due to anatomical variations between strains/genotypes. This model has a 25-30% mortality rate, peaking 2-4 days post-surgery, which can be minimized through proper pain management and postoperative monitoring. Rats received either saline or KXA (80 μL/kg) sublingually twice daily for 1, 2, or 4 weeks. Appearance, behavior, activity, diet, stool, weight, and respiratory symptoms were monitored throughout. All procedures were approved by the Ethics Committee of Tai'an Central Hospital (Approval No. 2023-06-51). At the end of the experiment, surviving rats were euthanized by intraperitoneal sodium pentobarbital injection (150 mg/kg) followed by cervical dislocation. Efforts to minimize animal suffering were made, including proper anesthesia, analgesia, and timely intervention for signs of distress.

Preparation of KXA-containing serum

Six SD rats were divided into control and treatment groups. The treatment group received KXA (80 $\mu L/kg)$ sublingually twice daily for three days. One hour after the final dose, arterial blood was collected, and serum was extracted and sterilized using a 0.22 μm filter membrane.

Echocardiography: At the end of the experiment, rats were anesthetized with 2% isoflurane, and cardiac function was assessed using a Vevo 2100 ultrasound system under doubleblind conditions. Parameters measured included left ventricular ejection fraction (LVEF), left ventricular fractional shortening (LVFS), left ventricular end-diastolic diameter (LVEDD), and left ventricular end-systolic dimension (LVESD). Image acquisition and analysis were performed

by two independent operators unaware of the grouping information. Group information was concealed in the image file names.

Hematoxylin and eosin (H&E) staining

Myocardial tissues (n=5) were fixed in 4% paraformaldehyde (Beyotime, Shanghai, China), embedded in paraffin, and sectioned. The sections were sequentially immersed in xylene and ethanol solutions, then stained using an H&E Staining Kit (Pinofei Biological, Wuhan, China). After dehydration and sealing, tissue morphology was examined under an optical microscope (Nikon, Tokyo, Japan) and scored blindly by two independent researchers. Six high-power fields were randomly selected for each section, and the average score was calculated to evaluate myocardial injury.

TUNEL staining

The One Step TUNEL Apoptosis Assay Kit (Beyotime) was used for TUNEL staining. Myocardial tissues (n=5) were dewaxed, hydrated, and treated with protease K for 15 minutes. After PBS washes, endogenous peroxidase was blocked for 20 minutes. The sections were incubated with TUNEL detection solution at 37°C for 60 minutes. For H9C2 cells, cells were fixed with 4% paraformaldehyde, incubated with 0.3% Triton X-100, and then treated with TUNEL detection solution for 60 minutes at 37°C. After PBS washing, sections and cells were sealed with anti-fluorescence quenching mounting medium and observed via fluorescence microscopy (Olympus, Tokyo, Japan) by two independent researchers. Five randomly selected fields at 40× magnification were used to calculate the percentage of TUNEL-positive cell nuclei.

ELISA assay

Rat serum (n=5) was harvested for the detection of N-terminal pro-B-type natriuretic peptide (NT-proBNP), suppression of tumorigenicity 2 (ST2), interleukin-6 (IL-6), tumor necrosis factor- α (TNF- α), matrix metalloproteinase-2 (MMP-2), and matrix metalloproteinase-9 (MMP-9) using commercially available ELISA kits (Elabscience, Wuhan, China). The assay was performed in triplicate, and the average value was calculated.

Table 1. Primers used in this study

Genes	5'> 3'
DLL-F	TGCCACTTCGGTTACAC
DLL-R	TGACACATTCGTTCCTCTC
Notch1-F	GATGGCCTCAATGGGTACAAG
Notch1-R	TCGTTGTTGTTGATGTCACAGT
Hes1-F	GTCCCCGGTGGCTGCTAC
Hes1-R	AACACGCTCGGGTCTGTGCT
GAPDH-F	AGATCCACAACGGATACATT
GAPDH-R	TCCCTCAAGATTGTCAGCAA

Quantitative real-time PCR (qPCR) assay

Total RNA was extracted using an RNA extraction kit (Vazyme, Nanjing, China) and quantified at 260 nm. cDNA synthesis was performed using the cDNA Synthesis Master Mix (Vazyme). Target gene quantification was performed using a real-time PCR system (Thermo Fisher Scientific, Massachusetts, USA) and a probebased qPCR mixture (Vazyme). GAPDH was used as the internal control, and data were analyzed using the $2-\Delta\Delta$ Ct method. Primer sequences are listed in **Table 1**.

Western blot

Total protein was measured using a protein quantitative assay kit (Beyotime) after extraction with RIPA lysis buffer (PHYGENE, Fuzhou, China). Following SDS-PAGE electrophoresis. proteins were transferred onto PVDF membranes (Merck) and blocked with bovine serum albumin (BSA; Bioswamp, Wuhan, China). The blots were probed with primary antibodies: anti-NOTCH1 (Cat No: 20687-1-AP, Proteintech, 1:1000), anti-DLL4 (Cat No: AF13221, Affinity, 1:1000), anti-NICD (Cat No: AF5307, Affinity, 1:1000), and anti-Hes1 (Cat No: ab108937, Abcam, 1:1000) for 12 hours at 4°C. After washing with TBST, the membranes were incubated with secondary antibodies: goat anti-rabbit (Cat No: RGAR001, Proteintech, 1:1000) and goat anti-mouse (Cat No: RGAM001, Proteintech, 1:1000) for 2 hours at room temperature. Membranes were then exposed to ECL Western Blotting Substrate (PHYGENE) and imaged using an iBright FL1500 Imaging System (Thermo Fisher Scientific). β-actin (Cat No: 81115-1-RR, Proteintech, 1:2000) served as the endogenous control. Each experiment was repeated three times.

Flow cytometry analysis

After euthanasia, blood and spleen tissues were collected. Spleen tissues were minced, filtered through 40 µm strainers, and subjected to RBC lysis (Thermo Fisher Scientific), followed by incubation with fluorochrome-conjugated antibodies: CD3-PE (BD Biosciences, 200003, USA), CD49b-APC (Abcam, ab41460, UK), CD4-APC (BD Biosciences, 201509), CD68-APC (Abcam, ab317758), F4/80-FITC (Thermo Fisher Scientific, AER-051-F), Ly6G-FITC (Abcam, ab25024), and CD11b-APC (Abcam, ab25482). Flow cytometry was performed using a MoFlo XDP cytometer (Beckman Coulter, California, USA), and data were analyzed using FlowJo7 software (Tree Star, Inc., Ashland, OR).

Cell culture

H9C2 cells (National Collection of Authenticated Cell Cultures) were cultured in DMEM with 10% FBS and 1% penicillin-streptomycin (Procell, Wuhan, China). Cells were treated with 5 µmol/L doxorubicin (Dox; MCE, USA) for 24 hours to induce myocardial injury, and then co-cultured with KXA-containing serum at varying concentrations for 24, 48, 72, and 96 hours to assess KXA's therapeutic effect [31].

Cell counting kit-8 (CCK-8)

Cell viability was assessed using the CCK-8 kit (Elabscience). Cells were plated in 96-well plates, and after the corresponding treatments, $10~\mu L$ of CCK-8 solution was added to each well. After 2 hours of incubation, absorbance at 450 nm was measured using a microplate reader (Thermo Fisher Scientific). The assay was performed in triplicate, and the average value was calculated.

Statistical analysis

Statistical analysis was performed using GraphPad Prism software (Version 8.0, USA). Data are presented as mean ± standard deviation (SD). Comparisons between two groups were performed using an independent samples t-test. Multiple group comparisons were conducted using one-way analysis of variance (ANOVA), followed by Tukey's post hoc test. A significance level of P<0.05 was considered statistically significant.

The cardioprotective role of Kuanxiong aerosol in post-myocardial infarction heart failure

Results

KXA alleviated HFAMI in rats

Echocardiographic assessments were conducted on various groups of rats. As expected, compared to the sham group, rats in the model group exhibited cardiac enlargement and thinning of the chamber walls (Figures 1A, S1). Additionally, the model group showed higher LVIDD and LVISD values, while the LVEF and LVFS were significantly lower than those in the sham group (Table 2). These findings confirmed that the HFAMI model was successfully established.

After KXA treatment for 1, 2, and 4 weeks, therapeutic efficacy improved in a time-dependent manner. No significant differences were observed between the 1-week and 2-week treatment groups and the model group. However, the 4-week treatment group exhibited the most notable improvement, showing significant recovery compared to the model group (Figures 1A, S1). Consistent with these results, LVIDD AND LVISD values were reduced, and LVEF and LVFS levels were significantly elevated in the 4-week treatment group (Table 2).

Histological analysis using H&E staining revealed that myocardial tissue from sham group rats had a well-preserved cellular structure, with orderly arrangement, distinct intercellular gaps, no edema, and no signs of inflammation or cell necrosis. In contrast, myocardial tissue from the model group rats showed significant damage, characterized by severe cell necrosis, blood vessel dilation, congestion, disordered myocardial cell arrangement, prominent interstitial edema, extensive inflammatory cell infiltration, vacuolar degeneration in the cytoplasm, and unclear nuclear membranes with severe chromatin condensation or aggregation.

Similar to the echocardiographic findings, myocardial injury in the 4-week KXA treatment group was notably alleviated compared to the model group, with marked improvements in necrosis, edema, and other indicators of myocardial damage (Figures 1B, S1). Furthermore, TUNEL staining revealed that the number of TUNEL-positive cells in the model group was significantly higher than in the sham group, while the 4-week KXA treatment group showed

a reduction in TUNEL-positive cells (**Figures 1C**, <u>S1</u>).

Additionally, ELISA was used to quantify cytokine levels in rat serum. As shown in **Figure 1D**, serum levels of NT-proBNP, ST2, IL-6, TNF- α , MMP2, and MMP9 were significantly elevated in the model group compared to the sham group. Remarkably, the 4-week KXA treatment effectively reversed these cytokine elevations (**Table 3**).

The effect of KXA on immune infiltration in rats with HFAMI

Having established that KXA modulates cytokine levels in serum, we next investigated its effects on immune cell infiltration. The ratios of neutrophils, macrophages, NK cells, and Th1 cells in rats treated with different interventions were evaluated by flow cytometry. As shown in Figure 2A-D, compared to the sham group, the model group exhibited elevated ratios of these immune cells. However, these ratios were significantly reduced following KXA treatment. These findings suggest that KXA ameliorates HFAMI by regulating immune cell infiltration.

Effect of KXA on the NOTCH1 pathway in rats with HFAMI

The NOTCH1 signaling pathway is critical in angiogenesis following myocardial infarction. To further investigate whether the regulatory effect of KXA in rats with HFAMI is related to the NOTCH1 pathway, we assessed the expression of Delta-like 4 (DLL4), Notch1, NOTCH intracellular domain (NICD), and hairy enhancer of split-1 (Hes1) in myocardial tissue. qPCR and Western blot analyses were performed on both infarcted and non-infarcted regions in the sham, model, and KXA groups. Compared to the sham group, the model group exhibited significantly reduced mRNA and protein expression of DLL4, Notch1, NICD, and Hes1 in both infarcted and non-infarcted areas, with more pronounced changes observed in the infarcted region (Figure 3A and 3B). In contrast, KXA treatment significantly increased the expression of these molecules in the infarcted myocardium compared to the model group (Figure 3A and 3B). These results suggest that KXA enhances the activation of the NOTCH1 pathway in rats with HFAMI.

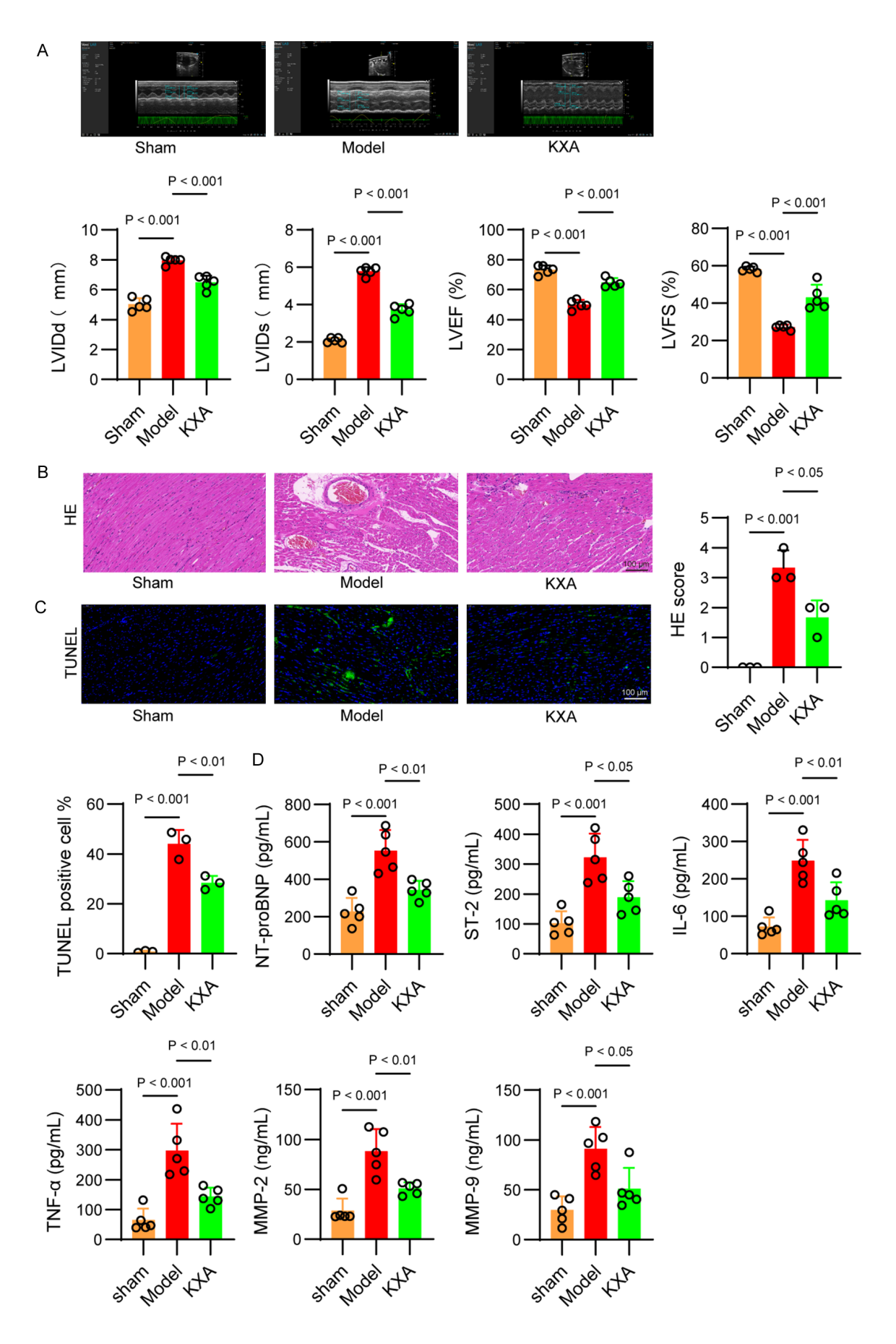


Figure 1. KXA alleviated heart failure after myocardial infarction in rats. A. Comparison of echocardiography at week 4 of rats in each group, n=5. B. Representative H&E-stained myocardial tissue from rats at week 4, n=3. C. Representative images of TUNEL staining of myocardial tissue at week 4, n=3. D. The contents of NT-proBNP, ST2, IL-6, TNF- α , MMP2 and MMP9 in serum of rats were determined by ELISA, n=5. Data were displayed as mean \pm SD.

Table 2. Effect of KXA on echocardiography in rats after myocardial infarction

	Sham			Model			KXA		
	Mean	P value	F value	Mean	P value	F value	Mean	P value	F value
LVIDD	5.03±0.37	/	9.558	7.95±0.23	<0.001	9.558	6.49±0.40	<0.001	9.558
LVIDS	2.09±0.12	/	8.932	5.78±0.21	<0.001	8.932	3.72±0.27	<0.001	8.932
LVEF (%)	73.17±2.75	/	9.412	49.98±2.79	<0.001	9.412	64.66±2.69	<0.001	9.412
LVFS (%)	58.23±1.26	/	7.503	27.26±1.10	<0.001	7.503	43.20±5.93	<0.001	7.503

KXA, Kuanxiong aerosol; LVEDD, Left ventricular end diastolic diameter; LVIDD, left ventricular end diastolic diameter; LVEF, Left ventricular ejection fraction; LVFS, Left ventricular fraction shortening.

Table 3. The levels of NT-proBNP, ST2, IL-6, TNF- α , MMP2 and MMP9 in serum of rats

Table 3. The levels of N1-proBNP, S12, IL-6, TNF-α, MMP2 and MMP9 in serum of rats											
	1 week										
		Sham		Model			KXA				
	Mean	P value	F value	Mean	P value	F value	Mean	P value	F value		
NT-proBNP	232.5±74.66	/	10.451	512.5±98.68	0.018	10.451	453.8±94.76	0.499	10.451		
ST2	112.1±39.82	/	12.008	321.3±76.33	0.014	12.008	222.1±72.46	0.178	12.008		
IL-6	82.54±21.74	/	5.781	223.6±54.52	0.014	5.781	212.9±54.16	0.821	5.781		
TNF-α	69.34±31.65	/	6.721	267.4±90.41	0.023	6.721	221.3±90.52	0.566	6.721		
MMP2	34.54±10.12	/	14.342	84.62±21.45	0.022	14.342	80.31±20.53	0.814	14.342		
MMP9	24.56±17.76	/	12.971	91.32±24.64	0.018	12.971	83.13±21.43	0.686	12.971		
					2 week						
		Sham		Model			KXA				
	Mean	P value	F value	Mean	P value	F value	Mean	P value	F value		
NT-proBNP	221.6±69.54	/	7.541	524.2±99.71	0.013	7.541	393.7±95.85	0.178	7.541		
ST2	109.6±33.77	/	8.845	318.4±82.36	0.015	8.845	212.6±74.38	0.174	8.845		

	Onam			IVIOGCI			1001		
	Mean	P value	F value	Mean	P value	F value	Mean	P value	F value
NT-proBNP	221.6±69.54	/	7.541	524.2±99.71	0.013	7.541	393.7±95.85	0.178	7.541
ST2	109.6±33.77	/	8.845	318.4±82.36	0.015	8.845	212.6±74.38	0.174	8.845
IL-6	77.43±22.83	/	6.088	237.2±57.46	0.011	6.088	198.8±50.17	0.432	6.088
TNF-α	67.71±34.55	/	12.874	271.7±92.31	0.023	12.874	197.8±83.52	0.362	12.874
MMP2	31.89±14.13	/	11.983	84.37±26.12	0.037	11.983	70.64±20.27	0.019	11.983
MMP9	27.43±16.63	/	9.753	91.14±23.54	0.019	9.753	74.11±20.16	0.395	9.753
	4 week								

	Sham			Model			KXA		
	Mean	P value	F value	Mean	P value	F value	Mean	P value	F value
NT-proBNP	227.8±73.76	/	8.821	553.8±109.6	<0.001	8.821	343.4±48.35	0.004	8.821
ST2	102.5±40.12	/	9.431	322.1±80.13	<0.001	9.431	189.6±53.77	0.012	9.431
IL-6	72.37±24.71	/	12.89	248.9±55.57	<0.001	12.89	142.5±48.48	0.007	12.89
TNF-α	64.87±38.56	/	7.067	297.3±89.24	<0.001	7.067	143.2±30.17	0.004	7.067
MMP2	28.69±12.23	/	10.482	88.31±22.19	<0.001	10.482	50.94±6.109	0.005	10.482
MMP9	29.65±13.86	/	9.328	91.03±21.94	<0.001	9.328	50.94±20.95	0.016	9.328

KXA, Kuanxiong aerosol; NT-proBNP, N-terminal pro B-type natriuretic peptide; ST2, Suppression of tumorigenicity 2; IL, Interleukin; TNF- α , Tumor Necrosis factor- α ; MMP, Matrix metalloproteinase.

KXA-containing serum modulates the NOTCH1 signaling pathway in cardiomyocyte apoptosis after MI

To further explore the therapeutic effects of KXA, we conducted *in vitro* experiments using

H9C2 cells treated with DOX to simulate MI. After exposure to DOX, the cells were treated with varying concentrations of KXA-containing serum. As expected, DOX treatment resulted in a substantial decrease in cell viability. However, KXA-containing serum enhanced cell viability in

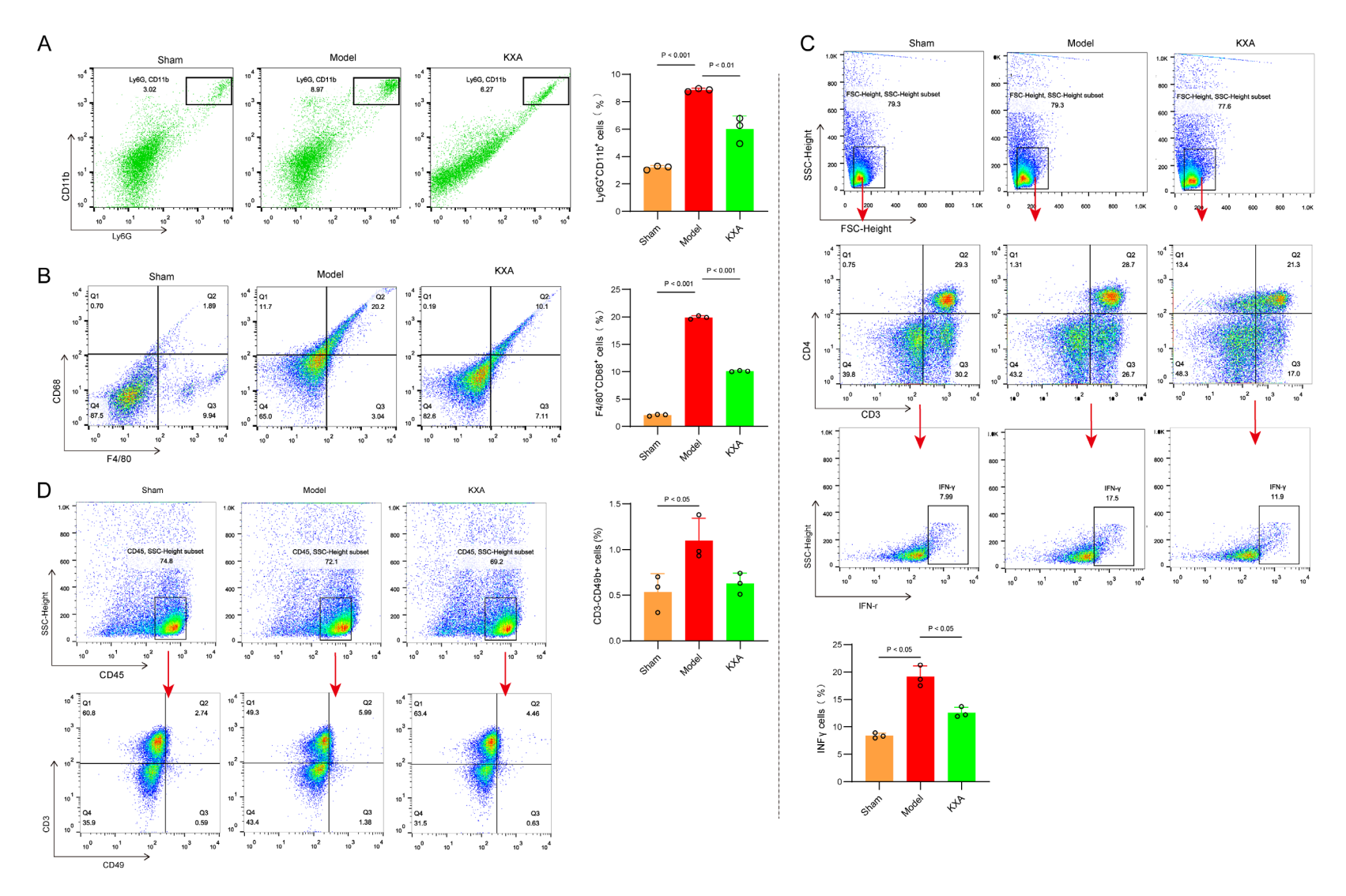


Figure 2. Effect of KXA on immune infiltration in rats with heart failure after myocardial infarction. A. The ratios of Neutrophil were detected by flow cytometry. B. The ratios of Macrophages was detected by flow cytometry. C. The ratios of NK cells was detected by flow cytometry. D. The ratios of Th1_cells was detected by flow cytometry. Data were displayed as mean ± SD. n=3.

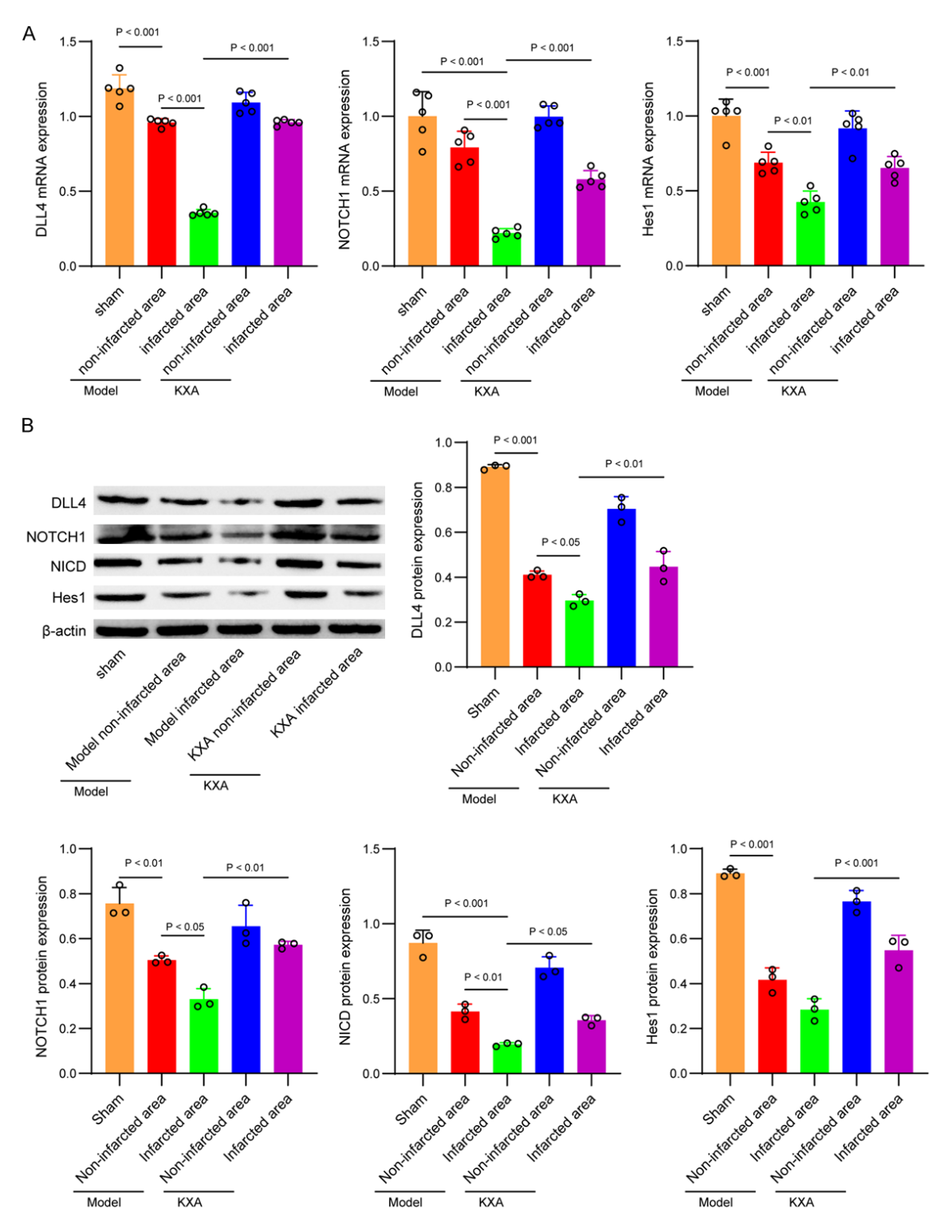
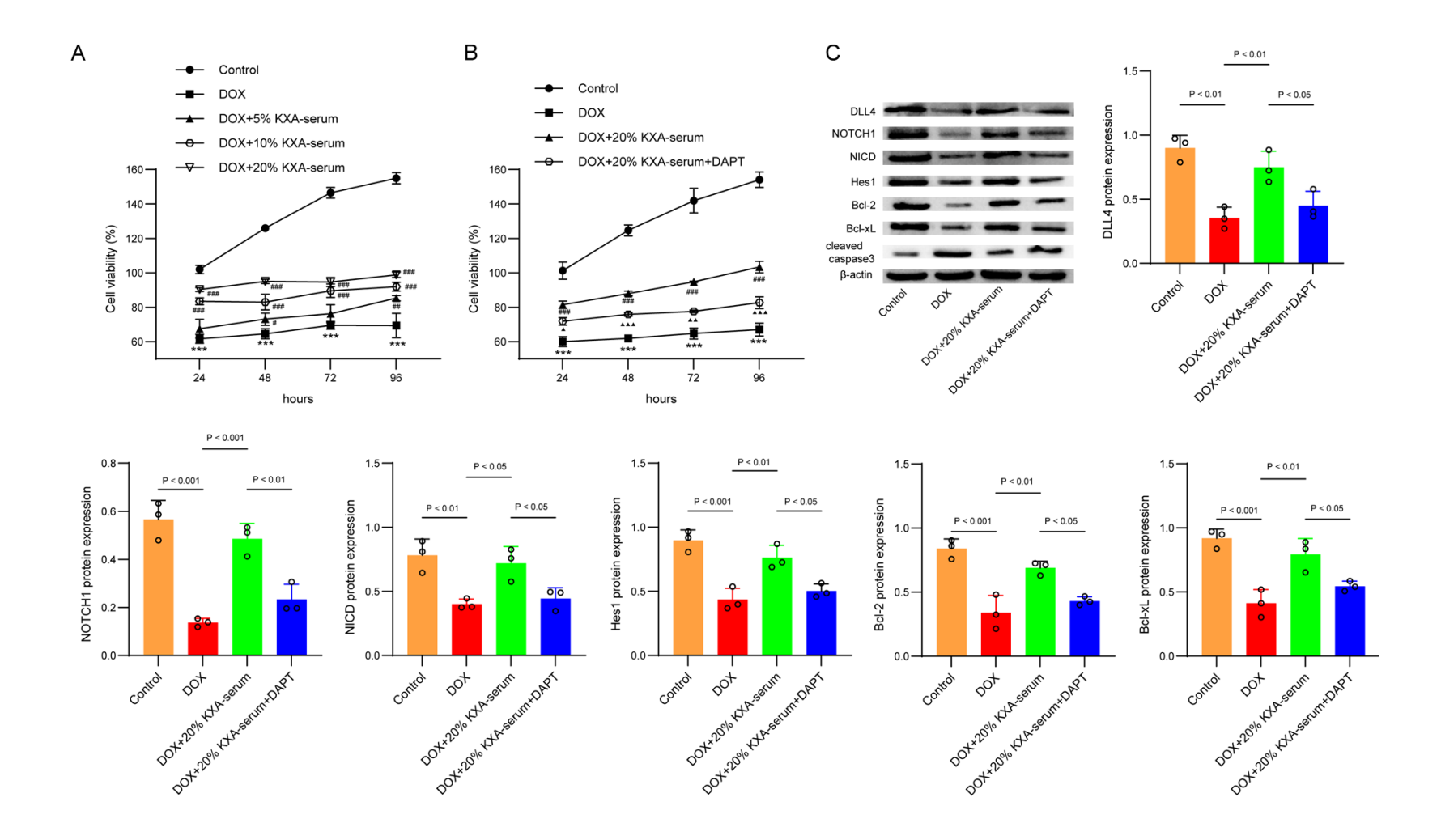


Figure 3. Effect of KXA on NOTCH1 pathway in rats with heart failure after myocardial infarction. A. qPCR assay was performed to detect the expression of DLL4, Notch1 and Hes1. B. Western blot was used to detect the expression of DLL4, Notch1, NICD and Hes1. Data were displayed as mean ± SD.

a concentration-dependent manner, with 20% KXA-containing serum showing the most pro-

nounced effect (**Figure 4A**). This concentration was selected for further experimentation.



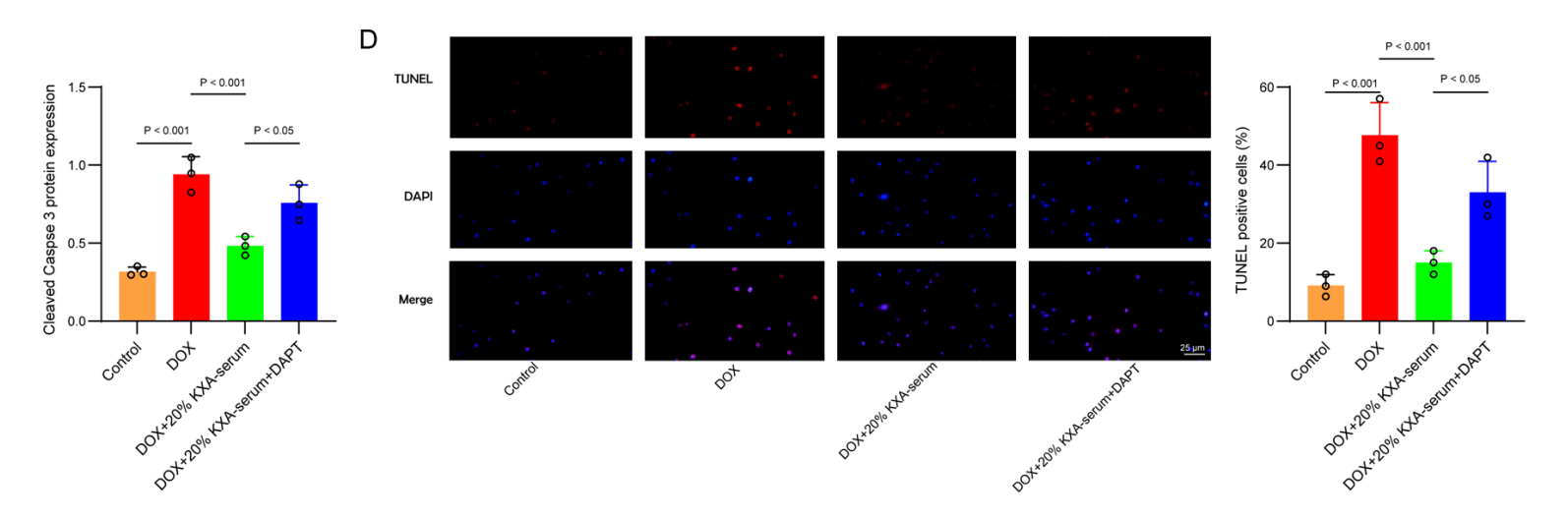


Figure 4. KXA-containing serum modulates the NOTCH1 signaling pathway in cardiomyocyte apoptosis after myocardial infarction. A. H9C2 cells were treated with doxorubicin in the presence or absence of different concentrations of KXA-containing serum (5%, 10% and 20%). The viability of H9C2 cells at 24 h, 48 h, 72 h and 96 h were determined by CCK-8. B-D. H9C2 cells were treated with doxorubicin in the presence or absence of 20% KXA-containing serum and NOTCH1 inhibitor (DAPT). B. The viability of H9C2 cells subjected to the treatment of 20% KXA-containing serum or NOTCH1 inhibitor (DAPT) at 24 h, 48 h, 72 h and 96 h were determined by CCK-8. C. The expressions of NOTHC1 pathway- and apoptosis-related proteins were determined by western blot. D. TUNEL staining was used to observe cell apoptosis. Data were displayed as mean ± SD. n=3. *P<0.05, **P<0.01, ***P<0.001.

To assess whether the effect of KXA was associated with the NOTCH1 pathway, we introduced DAPT, a NOTCH1 pathway inhibitor. As shown in Figure 4B, DAPT effectively reversed the positive effect of KXA-containing serum on cell viability in DOX-treated cells. Western blot analysis revealed that in the DOX group, the protein expression levels of DLL4, NOTCH1, NICD, Hes1, Bcl-2, and Bcl-xL were decreased. while cleaved caspase-3 levels were elevated (Figure 4C). These changes were partially reversed by 20% KXA-containing serum. However, DAPT treatment completely reversed the effects of KXA-containing serum (Figure 4C). Furthermore, TUNEL staining demonstrated a significant increase in TUNEL-positive cells in the DOX group compared to the control group. KXA-containing serum treatment significantly reduced the number of TUNEL-positive cells in DOX-treated cells (Figure 4D). Notably, this protective effect was abolished by DAPT co-treatment (Figure 4D).

Discussion

KXA is a clinically validated traditional Chinese medicine formulation with proven multi-pharmacological activities, including potent antioxidant effects through free radical scavenging, significant anti-inflammatory action via cytokine modulation, and notable sedative and analgesic properties that contribute to its therapeutic efficacy in cardiovascular conditions [11]. While KXA has been extensively used in clinical practice for managing angina pectoris and has shown promising cardioprotective effects in preliminary studies, its comprehensive therapeutic mechanisms in MI and subsequent HF development remain underexplored. Here, we conducted a systematic investigation to delineate the mechanistic foundations of KXA's therapeutic actions throughout the progression from acute MI to chronic HF.

We first established an in vivo rat model to assess the impact of KXA on cardiac function. Remarkably, our results demonstrated that KXA significantly improved cardiac functionality, corroborating previous reports of its cardioprotective effects [11]. Importantly, we identified the synergy between the pharmacological properties of KXA's constituent essential oils and their collective cardioprotective effects. For example, Younis et al. reported that sandal-

wood oil plays a key role in mitigating DOXinduced cardiotoxicity in vivo [32]. In addition, we observed that 4 weeks of KXA treatment significantly reduced serum levels of NT-proBNP, ST2, IL-6, TNF-α, MMP2, and MMP9 in model rats. Previous studies have shown that NT-proBNP serves as a diagnostic marker for acute MI, with elevated levels associated with poor outcomes in MI patients [33]. ST2, a biomarker for HF, contributes to myocardial fibrosis and ventricular remodeling when overexpressed [34]. Pro-inflammatory cytokines like IL-6 and TNF-α promote myocardial damage and dysfunction by modulating cardiomyocyte phenotype, making them critical therapeutic targets for HF [35]. MMP2 and MMP9, which regulate extracellular matrix degradation in cardiomyocytes, are important biomarkers for identifying individuals at risk of HF [36]. Collectively, these findings suggest that KXA exerts multifaceted therapeutic effects by modulating two key pathological processes in HF: inflammation and adverse ventricular remodeling.

Building upon our observations of KXA-mediated cytokine attenuation, we next investigated its immunomodulatory effects in HFAMI. Our comprehensive analysis revealed that KXA treatment significantly altered the cardiac immune landscape by reducing the infiltration of key pro-inflammatory immune cells, including neutrophils, macrophages, Th1 cells, and NK cells in HFAMI rats. This finding is significant, as neutrophils drive post-MI inflammation through mechanisms such as the release of pro-inflammatory cytokines, secretion of matrix-degrading metalloproteinases, and production of reactive oxygen species, all contributing to irreversible myocardial damage and maladaptive remodeling [37, 38]. Similarly, cardiac macrophages exhibit dramatic phenotypic changes during MI, with pro-inflammatory macrophage populations exacerbating tissue injury and impairing cardiac function [39]. These results underscore the role of immune system modulation in the progression of HF after MI. Our data indicate that KXA plays a critical role in regulating the immune microenvironment.

Mechanistic investigations revealed that KXA modulates the NOTCH1 signaling pathway, a critical regulator of lipid metabolism and inflam-

matory responses in cardiovascular diseases [40]. This is particularly relevant given that borneol, one of KXA's active components, has previously been shown to influence NOTCH1 signaling [29]. Using a NOTCH1 inhibitor, we confirmed that KXA's action on this pathway is specific. NOTCH1 activation involves canonical ligand-receptor interactions, where DLL4 binding to NOTCH1 induces the release of the NOTCH intracellular domain (NICD), which then activates downstream effectors like Hes1 [41]. Previous studies have reported downregulation of NOTCH1 and Hes1 in DOX-induced cardiac failure models [42]. Meanwhile, Cai et al. demonstrated that miR-455-5p triggers pathological cardiac remodeling by suppressing NICD release and the NOTCH1 signaling cascade [43]. Similarly, Onat et al. observed reduced expression of NOTCH1 signaling components (NOTCH1, Hes1, DLL4) in isoproterenol-induced MI rat models [44]. Consistent with these findings, we observed reduced expression of NOTCH1 signaling components in DOX-induced H9C2 cells, along with increased pro-apoptotic protein expression and decreased anti-apoptotic protein levels. Notably, KXA treatment alleviated these changes, and the effects were reversed by the NOTCH1 inhibitor, confirming that KXA regulates the immune system and exerts cardioprotective effects via NOTCH1 signaling.

In conclusion, our research, encompassing both animal and cellular experiments, highlights the therapeutic efficacy of KXA in HF following MI. Notably, this study underscores that KXA's cardioprotective effects are primarily mediated through activation of the NOTCH1 pathway and modulation of the immune microenvironment. Furthermore, this study supports the potential for inhalation administration at the animal level, offering insights for clinical application. This work also provides a theoretical basis for combining KXA with other drugs in clinical HF therapy. However, the study has some limitations, including reliance on a single animal model and the lack of comprehensive verification of signaling pathway interactions. Future studies should focus on efficacy and safety evaluations in mammalian models.

Disclosure of conflict of interest

None.

Abbreviations

KXA, Kuanxiong aerosol; HFAMI, Heart failure after myocardial infarction; TCM, Traditional Chinese medicine: LVEF, Left ventricular ejection fraction; LVFS, Left ventricular fraction shortening; LVEDD, Left ventricular end diastolic diameter; LVESD, Left ventricular end-systolic dimension; LVMI, Left ventricular mass index; H&E, Hematoxylin and eosin; TUNEL, Terminal deoxynucleotidyl transferase dUTP nick end labelling; ELISA, Enzyme-linked immunosorbent assay; NT-proBNP, N-terminal pro B-type natriuretic peptide; ST2, Suppression of tumorigenicity 2; IL, Interleukin; TNF-α, Tumor Necrosis factor-α; MMP, Matrix metalloproteinase; CCK-8, Cell counting kit-8; DLL4, Delta-like 4; NICD, NOTCH intracellular domain: Hes-1. Hairv enhancer of split-1; Bcl-2, B-cell lymphoma-2; Bcl-xL, B-cell lymphoma-extra-large.

Address correspondence to: Dr. Yingwu Liu, Department of Heart Center, Tianjin Third Central Hospital, No. 83 Jintang Road, Hedong District, Tianjin 300170, P. R. China. Tel: +86-15522242811; E-mail: liuyingwuzx@sina.com

References

- [1] Duggan JP, Peters AS, Trachiotis GD and Antevil JL. Epidemiology of coronary artery disease. Surg Clin North Am 2022; 102: 499-516.
- [2] Gerber Y, Weston SA, Enriquez-Sarano M, Berardi C, Chamberlain AM, Manemann SM, Jiang R, Dunlay SM and Roger VL. Mortality associated with heart failure after myocardial infarction: a contemporary community perspective. Circ Heart Fail 2016; 9: e002460.
- [3] Jia K, Cheng H, Ma W, Zhuang L, Li H, Li Z, Wang Z, Sun H, Cui Y, Zhang H, Xie H, Yi L, Chen Z, Sano M, Fukuda K, Lu L, Pu J, Zhang Y, Gao L, Zhang R and Yan X. RNA Helicase DDX5 maintains cardiac function by regulating Camkllδ alternative splicing. Circulation 2024; 150: 1121-1139.
- [4] Wu Q, Yao Q, Hu T, Yu J, Jiang K, Wan Y and Tang Q. Dapagliflozin protects against chronic heart failure in mice by inhibiting macrophage-mediated inflammation, independent of SGLT2. Cell Rep Med 2023; 4: 101334.
- [5] Bauersachs J, de Boer RA and Zieroth S. The year in cardiovascular medicine 2023: the top 10 papers in heart failure and cardiomyopathies. Eur Heart J 2024; 45: 507-509.
- [6] Wang A, Zhao W, Yan K, Huang P, Zhang H, Zhang Z, Zhang D and Ma X. Mechanisms and

- efficacy of traditional chinese medicine in heart failure. Front Pharmacol 2022; 13: 810587.
- [7] Shao-Mei W, Li-Fang Y and Li-Hong W. Traditional Chinese medicine enhances myocardial metabolism during heart failure. Biomed Pharmacother 2022; 146: 112538.
- [8] Zhang Z, Chen F, Wan J and Liu X. Potential traditional Chinese medicines with anti-inflammation in the prevention of heart failure following myocardial infarction. Chin Med 2023; 18: 28.
- [9] Wang J, Chen P, Cao Q, Wang W and Chang X. Traditional Chinese medicine ginseng dingzhi decoction ameliorates myocardial fibrosis and high glucose-induced cardiomyocyte injury by regulating intestinal flora and mitochondrial dysfunction. Oxid Med Cell Longev 2022; 2022: 9205908.
- [10] Yang M, Wu H, Qian H, Li D, Xu H, Chen J, Zhong J, Wu W, Yang H, Chen X, Min X and Chen J. Linggui Zhugan decoction delays ventricular remodeling in rats with chronic heart failure after myocardial infarction through the Wnt/β-catenin signaling pathway. Phytomedicine 2023; 120: 155026.
- [11] Zhang YZ, Zeng RX, Zhou YS and Zhang MZ. Kuanxiong aerosol in treatment of angina pectoris: a literature review and network pharmacology. Chin J Integr Med 2021; 27: 470-480.
- [12] Zhuang J, Dai X, Zhang H, Chen Y, Cai H, Jin Z, Zhong L and Chen B. A meta-analysis for Kuanxiong Aerosol on the treatment of angina pectoris. Am J Emerg Med 2020; 38: 1218-1225.
- [13] Lu Y, Yang ML, Shen AL, Lin S, Peng MZ, Wang TY, Lu ZQ, Wang YL, Peng J and Chu JF. Pharmacodynamic mechanism of kuanxiong aerosol for vasodilation and improvement of myocardial ischemia. Chin J Integr Med 2022; 28: 319-329.
- [14] Lu Y, Yang M, Peng M, Xie L, Shen A, Lin S, Huang B, Chu J and Peng J. Kuanxiong aerosol inhibits apoptosis and attenuates isoproterenol-induced myocardial injury through the mitogen-activated protein kinase pathway. J Ethnopharmacol 2021; 269: 113757.
- [15] Chen HJ, Chen YF, Chen JF, Qian K, Zhu YY, Fang L, Zhang Y, Yang T, Wang GW and Huang PT. Kuanxiong aerosol attenuates ischemic stroke injury via modulation of the TRPV1 channel. Chin J Integr Med 2025; [Epub ahead of print].
- [16] Vafadarnejad E, Rizzo G, Krampert L, Arampatzi P, Arias-Loza AP, Nazzal Y, Rizakou A, Knochenhauer T, Bandi SR, Nugroho VA, Schulz DJJ, Roesch M, Alayrac P, Vilar J, Silvestre JS, Zernecke A, Saliba AE and Cochain C. Dynamics of cardiac neutrophil diversity in murine

- myocardial infarction. Circ Res 2020; 127: e232-e249.
- [17] Swirski FK and Nahrendorf M. Cardioimmunology: the immune system in cardiac homeostasis and disease. Nat Rev Immunol 2018; 18: 733-744.
- [18] Kologrivova I, Shtatolkina M, Suslova T and Ryabov V. Cells of the immune system in cardiac remodeling: main players in resolution of inflammation and repair after myocardial infarction. Front Immunol 2021; 12: 664457.
- [19] Jiang H, Fang T and Cheng Z. Mechanism of heart failure after myocardial infarction. J Int Med Res 2023; 51: 1-15.
- [20] Li Y, Hu Y, Jiang F, Chen H, Xue Y and Yu Y. Combining WGCNA and machine learning to identify mechanisms and biomarkers of ischemic heart failure development after acute myocardial infarction. Heliyon 2024; 10: e27165.
- [21] Lv Y, Pang X, Cao Z, Song C, Liu B, Wu W and Pang Q. Evolution and function of the notch signaling pathway: an invertebrate perspective. Int J Mol Sci 2024; 25: 3322.
- [22] Dergilev KV, Zubkova ES, Beloglazova IB, Menshikov MY and Parfyonova EV. Notch signal pathway - therapeutic target for regulation of reparative processes in the heart. Ter Arkh 2018; 90: 112-121.
- [23] Aquila G, Kostina A, Vieceli Dalla Sega F, Shlyakhto E, Kostareva A, Marracino L, Ferrari R, Rizzo P and Malaschicheva A. The notch pathway: a novel therapeutic target for cardiovascular diseases? Expert Opin Ther Targets 2019; 23: 695-710.
- [24] Peng X, Wang S, Chen H and Chen M. Role of the Notch1 signaling pathway in ischemic heart disease (Review). Int J Mol Med 2023; 51: 27.
- [25] Kachanova O, Lobov A and Malashicheva A. The role of the notch signaling pathway in recovery of cardiac function after myocardial infarction. Int J Mol Sci 2022; 23: 12509.
- [26] Cui LG, Wang SH, Komal S, Yin JJ, Zhai MM, Zhou YJ, Yu QW, Wang C, Wang P, Wang ZM, Zafar AM, Shakeel M, Zhang LR and Han SN. ALKBH5 promotes cardiac fibroblasts pyroptosis after myocardial infarction through Notch1/ NLRP3 pathway. Cell Signal 2025; 127: 111574.
- [27] Zhang W, Xu H, Li C, Han B and Zhang Y. Exploring Chinese herbal medicine for ischemic stroke: insights into microglia and signaling pathways. Front Pharmacol 2024; 15: 1333006.
- [28] Hong Y, Wang H, Xie H, Zhong X, Chen X, Yu L, Zhang Y, Zhang J, Wang Q, Tang B, Lu L and Guo D. Qishen Granule protects against myocardial ischemia by promoting angiogenesis

- through BMP2-DII4-Notch1 pathway. Chin Herb Med 2024; 17: 139-147.
- [29] Ma R, Lu D, Xie Q, Yuan J, Ren M, Li Y, Wang J, Li J, Xu Z and Wang J. I-Borneol and d-Borneol promote transdifferentiation of astrocytes into neurons in rats by regulating Wnt/Notch pathway to exert neuroprotective effect during recovery from cerebral ischaemia. Phytomedicine 2023; 109: 154583.
- [30] Lugrin J, Parapanov R, Krueger T and Liaudet L. Murine myocardial infarction model using permanent ligation of left anterior descending coronary artery. J Vis Exp 2019.
- [31] Zhao L, Qi Y, Xu L, Tao X, Han X, Yin L and Peng J. MicroRNA-140-5p aggravates doxorubicininduced cardiotoxicity by promoting myocardial oxidative stress via targeting Nrf2 and Sirt2. Redox Biol 2018; 15: 284-296.
- [32] Younis NS. Doxorubicin-induced cardiac abnormalities in rats: attenuation via sandalwood oil. Pharmacology 2020; 105: 522-530.
- [33] Shen S, Ye J, Wu X and Li X. Association of Nterminal pro-brain natriuretic peptide level with adverse outcomes in patients with acute myocardial infarction: a meta-analysis. Heart Lung 2021; 50: 863-869.
- [34] Riccardi M, Myhre PL, Zelniker TA, Metra M, Januzzi JL and Inciardi RM. Soluble ST2 in heart failure: a clinical role beyond B-type natriuretic peptide. J Cardiovasc Dev Dis 2023; 10: 468.
- [35] Hanna A and Frangogiannis NG. Inflammatory cytokines and chemokines as therapeutic targets in heart failure. Cardiovasc Drugs Ther 2020; 34: 849-863.
- [36] Radosinska J, Barancik M and Vrbjar N. Heart failure and role of circulating MMP-2 and MMP-9. Panminerva Med 2017; 59: 241-253.
- [37] Daseke MJ 2nd, Chalise U, Becirovic-Agic M, Salomon JD, Cook LM, Case AJ and Lindsey ML. Neutrophil signaling during myocardial infarction wound repair. Cell Signal 2021; 77: 109816.

- [38] El Kazzi M, Rayner BS, Chami B, Dennis JM, Thomas SR and Witting PK. Neutrophil-mediated cardiac damage after acute myocardial infarction: significance of defining a new target cell type for developing cardioprotective drugs. Antioxid Redox Signal 2020; 33: 689-712.
- [39] Dick SA, Macklin JA, Nejat S, Momen A, Clemente-Casares X, Althagafi MG, Chen J, Kantores C, Hosseinzadeh S, Aronoff L, Wong A, Zaman R, Barbu I, Besla R, Lavine KJ, Razani B, Ginhoux F, Husain M, Cybulsky MI, Robbins CS and Epelman S. Self-renewing resident cardiac macrophages limit adverse remodeling following myocardial infarction. Nat Immunol 2019; 20: 29-39.
- [40] Lee HJ, Kim MY and Park HS. Phosphorylationdependent regulation of Notch1 signaling: the fulcrum of Notch1 signaling. BMB Rep 2015; 48: 431-437.
- [41] Zhu P, Chen C, Wu D, Chen G, Tan R and Ran J. AGEs-induced MMP-9 activation mediated by Notch1 signaling is involved in impaired wound healing in diabetic rats. Diabetes Res Clin Pract 2022; 186: 109831.
- [42] Merino H and Singla DK. Notch-1 mediated cardiac protection following embryonic and induced pluripotent stem cell transplantation in doxorubicin-induced heart failure. PLoS One 2014; 9: e101024.
- [43] Cai S, Chang J, Su M, Wei Y, Sun H, Chen C and Yiu KH. miR-455-5p promotes pathological cardiac remodeling via suppression of PRMT1mediated Notch signaling pathway. Cell Mol Life Sci 2023; 80: 359.
- [44] Onat E, Önalan E, Özdem B, Kavak Balgetir M and Kuloğlu T. Effect of humanine on the Notch signaling pathway in myocardial infarction. Turk J Med Sci 2023; 53: 1658-1666.

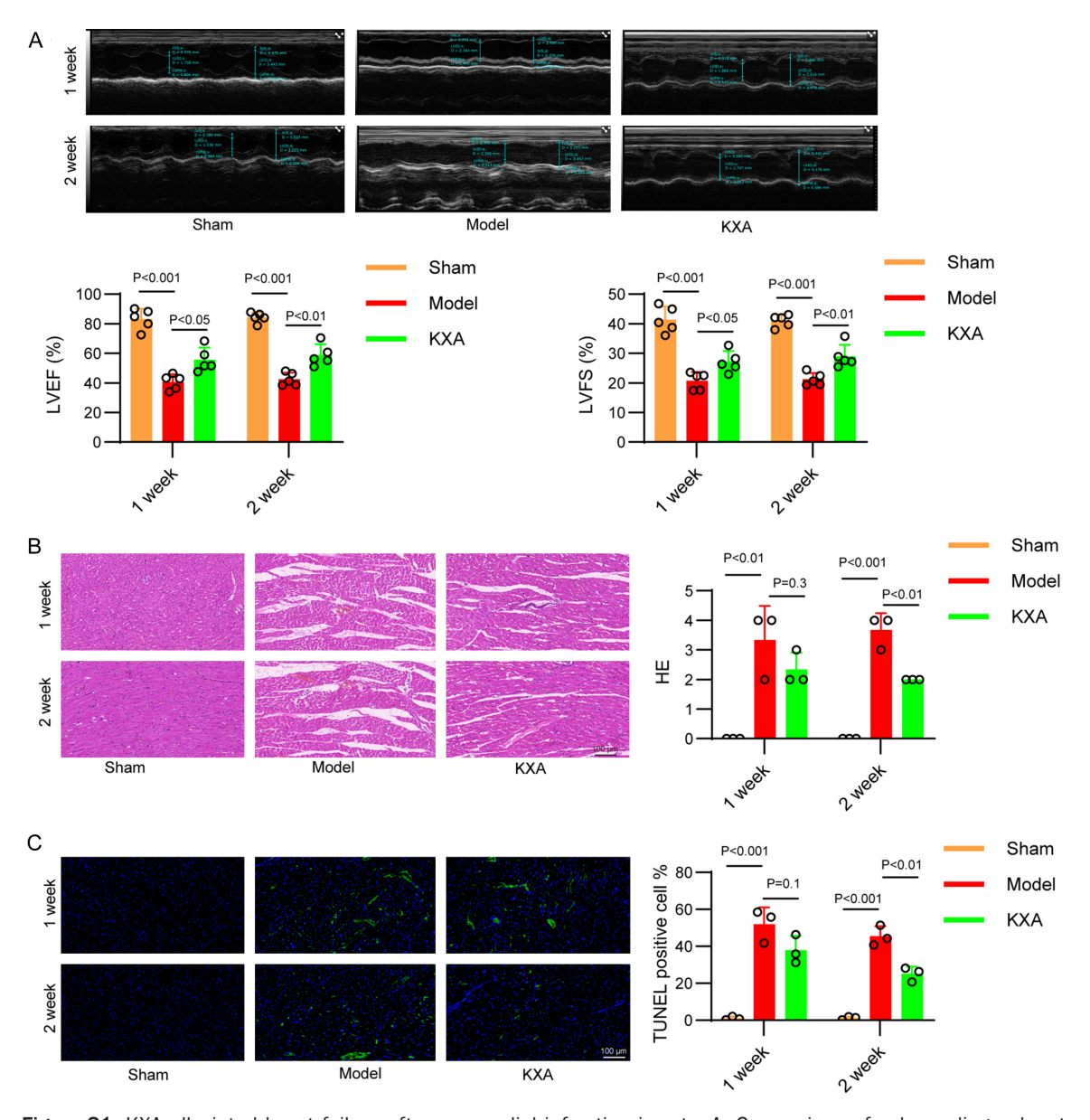


Figure S1. KXA alleviated heart failure after myocardial infarction in rats. A. Comparison of echocardiography at week 1 and 2 of rats in each group, n=5. B. Representative H&E-stained myocardial tissue from rats at week 1 and 2, n=3. C. Representative images of TUNEL staining of myocardial tissue at week 1 and 2, n=3.